



## Role of tool rotational speed on the tribological characteristics of magnesium based AZ61A/TiC composite developed via friction stir processing route

P. Sagar <sup>a,\*</sup>, A. Handa <sup>b</sup>

<sup>a</sup> Ph.D Research Scholar, I.K. Gujral Punjab Technical University, Kapurthala, India

<sup>b</sup> Department of Mechanical Engineering, I.K. Gujral Punjab Technical University, Kapurthala, India

\* Corresponding e-mail address: jasujaprem@gmail.com

ORCID identifier:  <https://orcid.org/0000-0003-2804-9458> (P.S.)

### ABSTRACT

**Purpose:** A new composite material was prepared and Different properties such as hardness and tribological behaviour of the fabricated metal matrix composite (MMC) was investigated and compared with the base AZ61A magnesium alloy.

**Design/methodology/approach:** For the current research work, state-of-the-art technology, Friction stir processing (FSP) was performed to develop magnesium based AZ61A/TiC composite at optimized set of machine parameters.

**Findings:** Increasing tool rotational speed ultimately leads in enhanced hardness, which further gives superior tribological properties as compared to base AZ61A alloy. Wear observations suggests a combination of abrasive and adhesive wear mechanism.

**Research limitations/implications:** More microstructural and mechanical properties can be examined.

**Practical implications:** The idea behind selecting AZ61A is mainly due to its increasing use in bicycle pedals and military equipment's where at certain places it needs to encounter friction. In this current work, microhardness study and wear behaviour of AZ61A/TiC composite processed via FSP were examined.

**Originality/value:** Paper is completely new and no work has been done till date considering this material and preparing composite with nanoparticles TiC.

**Keywords:** Friction stir processing, AZ61A magnesium alloy, Microhardness, Wear

**Reference to this paper should be given in the following way:**

P. Sagar, A. Handa, Role of tool rotational speed on the tribological characteristics of magnesium based AZ61A/TiC composite developed via friction stir processing route, Journal of Achievements in Materials and Manufacturing Engineering 101/2 (2020) 60-75. DOI: <https://doi.org/10.5604/01.3001.0014.4921>

### PROPERTIES

## 1. Introduction

There is an increasing interest in lightweight, maximum performance, eco-friendly and low-emission vehicles. In this respect, magnesium is being increasingly preferred over aluminium not just for its 66% lower density but also for its higher strength to weight ratio [1]. In addition, magnesium constitutes almost 2.7% of the earth's crust, is the sixth most abundant element in the earth's crust and third most abundant dissolved mineral in seawater [1]. In spite of these advantages, insufficient hardness and relatively poor protection from wear constraints the extensive use magnesium alloys. To enhance its mechanical properties, a specific percentage of secondary phase reinforce particles is required to be incorporated with the base magnesium or its alloys to produce magnesium matrix composites (MMC). Various manufacturing techniques have been studied such as Mukhin et al. [2] used diffusion bonding to fabricate composites of YAG, Yb:YAG, Yb:GGG, and TGG crystals, Bodukuri et al. [3], Jiang et al. [4], and Schubert et al. [5] fabricated Al-SiC-B<sub>4</sub>C MMC, reinforced MMC and copper based composites by powder metallurgy. Also *in situ* fabrication [6], spray deposition [7], stir and squeeze casting [8-11] and vapor deposition methods have been adopted by researchers to fabricate bulk MMCs [12-13]. All these manufacturing processes of developing composites transform the material from solid to liquid phase.

On the flip side, the techniques which do not have a phase change process such as solid state processing entails many merits over conventional phase change techniques. Novel, Friction stir processing (FSP) operates on the friction stir welding principle (FSW) [14]. Stirring action of FSP has been successfully used to disperse secondary phase particles in the parent metal and producing the next generation materials such as MMCs [15,16]. In the most recent times, various researchers have utilized the FSP procedure to improve wear and hardness of these MMCs. Reddy et al. [17] incorporated SiC and B<sub>4</sub>C particles through hole filling approach into the upper surface of magnesium base ZM21 alloy to develop a surface composite. It was found that there was no formation of intermetallic compounds and a strong bond was formed between carbide particles and the metal matrix. Furthermore, they investigated properties such as microhardness and dry sliding wear on the developed composite. They found similar values of hardness of base metal and FSPed alloy without reinforced particles. ZM21/B<sub>4</sub>C composite demonstrated higher values of hardness compared to ZM21/SiC. As far as the wear properties are concerned, adhesive wear mechanism was observed and it was presumed that almost 70% wear opposition for ZM21/B<sub>4</sub>C was obtained in contrast with the base metal.

Aabbsi et al. [18] developed two surface composites namely, AZ91/SiC and AZ91/Al<sub>2</sub>O<sub>3</sub> via groove filling approach. Wear, mechanical properties, and corrosion resistance were examined and compared with as cast AZ91. The AZ91/SiC developed higher values of hardness, ultimate tensile strength, and percent elongation compared to AZ91/Al<sub>2</sub>O<sub>3</sub> and base metal, which was attributed to the increase in number of passes. The wear test was conducted as per ASTM G99 standard on TRI-PIN-ON-DISK equipment using a stainless steel disk as a counter face along with a sliding speed of 1 mm s<sup>-1</sup>, contact force of 50 N, and total distance of 500 m. Cylindrical pins with 5 mm diameter and 40mm height were prepared from the samples using wire cut machine. They concluded that the wear rate for AZ91/SiC and AZ91/Al<sub>2</sub>O<sub>3</sub> was almost same but superior to the base metal. Singh et al. [19] introduced TiC reinforced particles into the blind holes drilled on AZ91 magnesium alloy surface to develop MMC via FSP. Wear performance was examined using pin-on-disc wear testing with two loads of 5 N and 10 N and resulting wear rate for these loads were examined. Rectangular pin specimens with cross sectional dimensions of 5 mm x 5 mm and 10 mm in length were machined from the as cast as well as FSPed AZ91 alloy for the wear tests. The counter face material used was a stainless steel disc with hardness value of nearly 220 Hv. Wear test were conducted and it was found that FSPed samples exhibited lower wear rate and higher wear resistance in contrast with as cast AZ91. Similarly, Arora et al. [20] investigated the tribological characteristics of AZ31/TiC composite as fabricated via FSP. Experimentation with single pass FSP process along with undersurface cooling was executed. Microhardness and wear test results concluded that the composite with single pass and undersurface cooling demonstrated enhanced microhardness and lesser wear rate. Arora et al. [21] compared wear behaviour of as cast AE42 magnesium alloy with FSPed AE42 samples. The authors concluded that FSPed AE42 alloy demonstrated decreased wear rate and enhanced hardness which was attributed to grain refinement. Furthermore, this study concluded that at low velocity and higher loads, surface delamination, plastic deformation and abrasive wear existed. Ram et al. [22] used pure magnesium and reinforced SiC particles to develop a novel composite via FSP. Enhanced microhardness of up to 45% and lower wear rate up to 47% was achieved. Finally, for the as cast, composite abrasive wear mechanism was found to be the dominant factor. Azizieh et al. [23] synthesized AZ31/Al<sub>2</sub>O<sub>3</sub> nanocomposite and examined the response of various parameters on hardness and wear behaviour. Authors considered varying tool rotation speeds of 800, 1000, 1200 and 1400 rpm with fixed tool transverse speed of 45 mm/min

and 2° tool tilt angle. It was found that due to refined grain formation, hardness increased from 50 Hv to 90 Hv and wear rate at 1000 and 1200 rpm was higher compared to that 800 rpm. Faraji and Asadi [24] in another study fabricated AZ91/Al<sub>2</sub>O<sub>3</sub> and obtained three times lower wear rate in contrast to the base metal. Recently, Dinaharan et al. [25] used fly ash to develop AZ31 magnesium base composite via processing route of stir cast and FSP. They obtained grain size of up to 4 μm and 33% lower wear rate for FSP compared to stir cast. In addition, they claimed superior wear resistance and microhardness of the composite developed via FSP. Very recently, Patle [26] examined sliding wear behaviour of as fabricated AZ91/B<sub>4</sub>C via FSP route. They found that the addition of B<sub>4</sub>C particles could enhance hardness of base metal, and leads to lower wear rate. They observed abrasive, severe adhesive, oxidative and delamination as major wear mechanisms at two different sliding velocities.

Literature survey shows that very little work has been carried out studying tribological behaviour of magnesium based AZ61A/TiC composite and compared with AZ61A magnesium alloy. The idea behind selecting AZ61A was mainly due to its increased use in bicycle pedals and military equipment where it needs to encounter friction

[27-29]. In this work, microhardness study and wear behaviour of AZ61A/TiC composite processed via FSP was conducted.

## 2. Experimental details

### 2.1. As received material

In this work, plates of magnesium, alloy AZ61A with dimensions of 200 mm×100 mm×6 mm were used. Table 1 presents the complete configuration of parent AZ61A magnesium alloy.

### 2.2. Reinforce particles

Nano titanium carbide (n-TiC) with 80 nm average particle sizes and 99.99% purity were used for the current study. Whereas Figure 1 represents Scanning electron microscopy (SEM), Energy-dispersive X-ray spectroscopy (EDSX) and X-ray diffraction (XRD) results obtained for nano reinforcement used in experiment. Table 2 presents the atomic and weight percentage of nano TiC reinforcement particles.

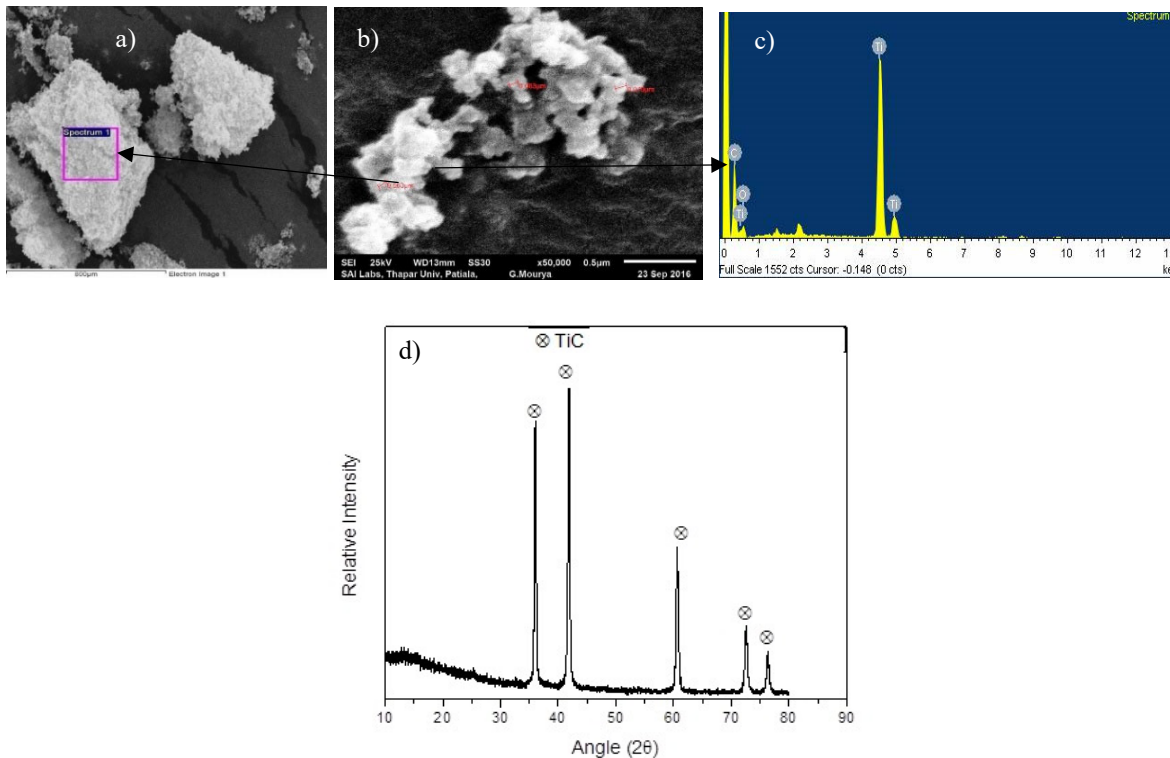


Fig. 1. a) SEM image of TiC powder, b) SEM image showing the average grain size, c) EDS spectra showing abundance of TiC particles, d) XRD image of TiC powder

Table 1.  
Chemical composition of as supplied magnesium AZ61A alloy

Element	Aluminium	Zinc	Manganese	Silicon	Iron	Copper	Nickel	Magnesium
Actual content, %	6.26	0.78	0.27	0.032	0.0021	0.011	0.0026	-----
Allowable range of content, %	5.8-7.2	0.4-1.5	0.15-0.50	0.05	0.005	0.05	0.005	Balance

Table 2.  
Chemical composition of secondary phase TiC particles

Element	C K	O K	Ti K	Final %
Weight, %	35.86	17.15	46.99	100 %
Atomic, %	59.25	21.28	19.47	100 %

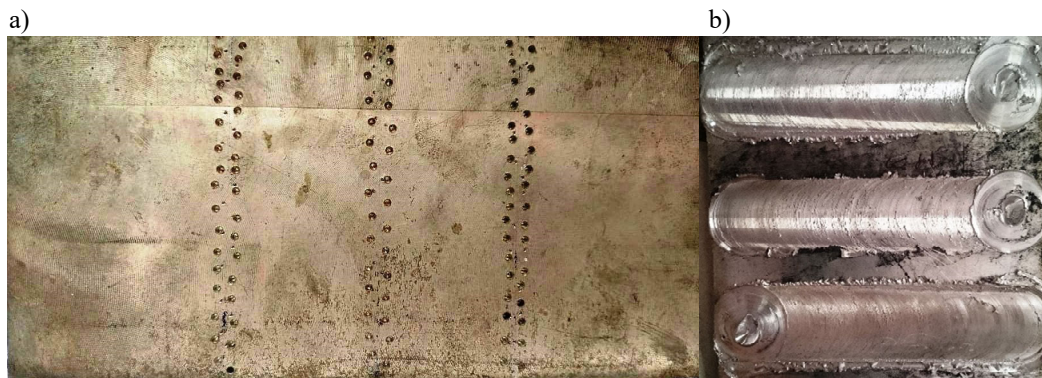


Fig. 2. a) Design sequence of blind holes made into AZ61A plate; b) pictorial view of FSPed surface

### 2.3. Fabrication of composite

Firstly, to consolidate the secondary phase particles, a grid of blind holes in zig-zag pattern with size  $\text{Ø}2 \text{ mm} \times 4 \text{ mm}$  were injected into the plate as shown in Figure 2. FSP was implemented using two high carbon high chromium (HCHCr) tools. The first tool had a shoulder but no pin was employed to cover the top of the holes after implanting TiC powder into the holes to prevent the scattering of particles during FSP. The second tool had a triangular pin profile with a shoulder diameter of 16 mm, making root diameter 6 mm and pin length 4 mm. Figure 2 (b) shows the pictorial view of the crown surface appearance of FSPed surfaces. Nearly 21 % of volume fraction of TiC was added as theoretically calculated by using formula [30].

Theoretical volume fraction = (Total volume of reinforcement particles / Total volume of the processing zone)  $\times 100$

Total volume of reinforcement particles = Numbers of holes  $\times$  Volume of each blind hole

Volume of cylindrical hole =  $\pi r^2 \times$  Depth of hole

Total volume of the processing zone = Working length  $\times$  Pin Length Tool  $\times$  Shoulder diameter

Six samples were prepared through FSP under various conditions as shown in Table 3. FSP experiments were conducted utilizing a modified dedicated vertical milling machine.

Table 3.  
Processing parameters for FSP of AZ61A/TiC

Parameter	Value 1	Value 2	Value 3
Tool rotation speed, rpm	800	1000	1200
Transverse speed, mm/min	40	40	40
No. of passes	3	3	3

### 2.4. Microstructure and microhardness test

The standard metallurgical practice were carried out to prepare the processed specimens. The specimens for optical microscopy were prepared by particular polishing with varying grit size SiC. Double disc polishing machine was used for mechanical polishing with emery papers of size 80,

100, 150, 220, 320, 500, 800, 1000, 1500 and 2000, respectively and with water as a lubricant. Further polishing was carried out with diamond paste. Polished specimens were then etched by 100 ml ethanol, 5 gm picric acid, 4 ml acetic acid, and 10 ml water for 15-20 sec. Prepared specimens than examined under image analysing software attached with the microscope which construct the grain boundaries completely and measured the grain size. For better results, all the optical images were taken within 25 minutes of sample preparation.

Microstructure investigations were done using optical microscopy (OM- Leica, Germany make) and measurement of microhardness was done by Vickers indentation method by applying a total load of 500gm for a dwell time of 15 sec. as per ASTM specifications. Hardness values were examined along a horizontal line underneath 1.5 mm from top surface at equal intervals of 0.5 mm between adjacent points. A total of thirty-three values were taken for a distance of 8 mm to the either side of the central line passing through stir zone. At every indentation point, three values were taken and mean value was considered.

**2.5. Wear test**

Machine and experiment detail

For examining wear and friction characteristics, pins of size Ø3 mm × 30 mm were prepared from base metal and from composites via wire cut electric discharge machining. All the experiments were done as per ASTM G99 standard and were examined using pin-on-disc tribotester (DUCOM

TR-20 LE), as shown schematically in Figure 3. Basic geometry of pin and disc is presented in Figure 4.

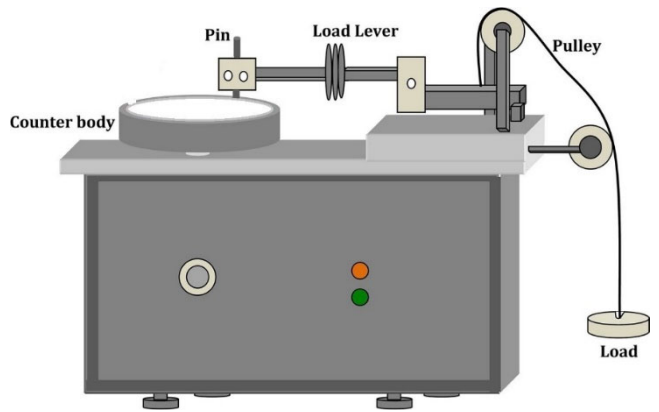


Fig. 3. Pictorial view of pin-on-disc tribotester [31]

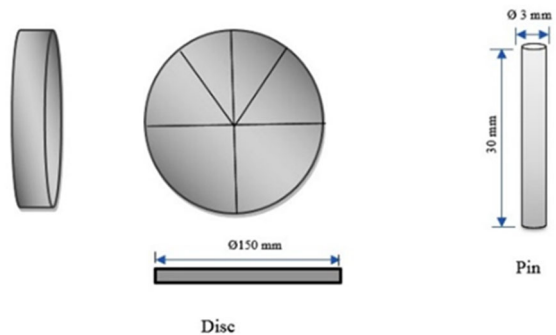


Fig. 4. Basic geometry of pin and disc

Table 4.

Final wear rate of composite as well base metal at various FSP conditions

	RPM	TS (mm/min)	LOAD (N)	Initial height (IH)	Final Height (FH)	Change in height ( $\Delta h=IH-FH$ )	Volumetric loss (VL)= $\pi r^2 \Delta h$ (mm <sup>3</sup> )	Wear rate =VL/S.D (mm <sup>3</sup> /m)
Composite	800	40	10	30	29.56916	0.43084	3.04539254	0.006090785
	800	40	20	30	29.41379	0.58621	4.14362538	0.008287251
	1000	40	10	30	29.38102	0.61898	4.37526013	0.00875052
	1000	40	20	30	29.28752	0.71248	5.03616488	0.01007233
	1200	40	10	30	29.43218	0.56782	4.01363567	0.008027271
	1200	40	20	30	29.34579	0.65421	4.62428338	0.009248567
Base metal			10	30	29.28452	0.71548	5.05737038	0.010114741
Base metal			20	30	29.057265	0.94273	6.66372234	0.013327445

Steel disc (EN31) of hardness of 60 HRC was used as a counter surface and prepared by silicon carbide papers of grit size 800 and 1000 preceded by acetone cleaning. All wear analysis was conducted for sliding distance of 500 m, time 600s, disc rpm 400, and varying load of 10 and 20 N. Volumetric loss was determined as a function of loss of height multiplying it with the cross-sectional area of pin. Further wear rate was calculated considering volumetric loss as a function of the sliding distance. Worn surfaces and the underlying wear mechanism were analyzed by scanning electron microscopy (JEOL, JSM-F100). Final values of calculated wear rate are presented in Table 4.

### 3. Results and discussion

#### 3.1. Microstructure and microhardness

The obtained microstructures of monolithic AZ61A and FSPed processed specimens are shown in Figure 5 and Figure 6. Figure 5 shows the optical micrographs of the as received AZ61A magnesium base alloy. The typical microstructure of AZ61A alloy is characterized by coarse  $\beta$ -Mg<sub>17</sub>-Al<sub>12</sub> and  $\alpha$ -Mg compound with discontinuous network at grain boundary. It was observed that unrefined coarse grains were distributed in the metal matrix. Additionally, clusters of small crystals were observed alongside segregated large crystals. The average grain size of the base was about 75  $\mu$ m.

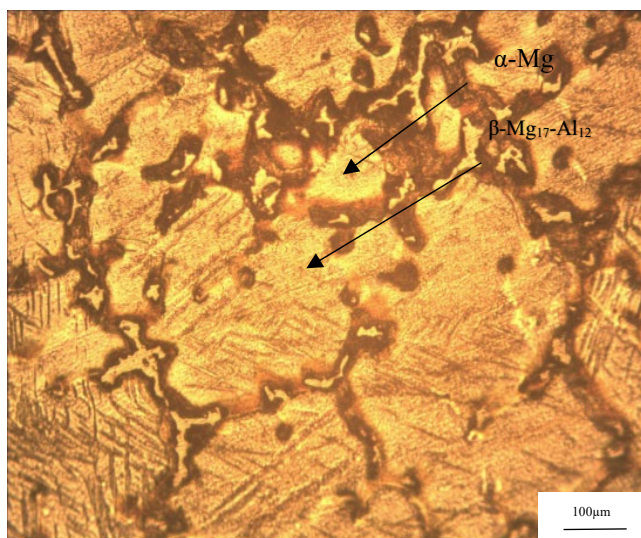


**Figure 5.** Optical micrograph of monolithic AZ61A base metal

AZ61A magnesium alloy incorporated with secondary phase TiC particles and further processed at various tool rotation speed. The specimen shows that coarse magnesium grains were not able to handle rigorous action of tool and broke up into tiny grains. Figure 6, presents microstructure images of different zones at 200 X. In almost all the specimens, stir zone (SZ) exhibited finer grains, which may be attributed to dynamic recrystallization, and heat generation, which is in agreement with several other studies [32-36]. In Figure 6, FSPed specimen processed at 800 rpm showed refined microstructure up to 3  $\mu$ m that may be due to nucleation of TiC and pinning of grain boundaries with nano reinforce particles. In addition fixed volume fraction of nano reinforce particles achieves better distribution and results in developing obstacles to growing grain boundary, which is in tune with Azizieh et. al [37]. In case of tool speed of 1000 rpm the OM reveals refined grains (up to 4.3  $\mu$ m) at stir zone as shown in Figure 6. However, at some places agglomeration was noticed which can be attributed to improper distribution of secondary phase particles in metal flow. As tool rotation speed increased to 1200 rpm, the microstructure images reveal that as heat input increased the grain growth (up to 5  $\mu$ m) occurred consequently larger grains were noticed at this parameter, which is in agreement with [37,38]. However, simultaneously shattering effect of rotation cause uniform distribution of secondary phase particle.

#### Microhardness

Microhardness values of the FSPed specimens was examined along the horizontal line passing through stir zone of cross section and presented in Figure 7. As received base metal AZ61A bore hardness of 60 HV. The hardness of the stir zone for all FSPed samples was considerably higher in contrast to the base magnesium alloy. This may be attributed to refined and small sized grains at the stir zone due to dynamic crystallization of FSP. As per the Hall-Petch equation, the grain size holds an inverse relationship with hardness. As grain size decreases, the hardness increases. Additionally, Orowan strengthening mechanism contribution that influence dislocation of grains in reinforced metal matrix composites. At higher rotational speed 1200 rpm, heat input increases and grain growth occur that consequently results in low hardness, as detailed by Azizieh et. al [23]. Hence as tool rotational speed increases, the microhardness of the composite decreases, these findings are in confirmation with the findings of Sathiskumar et. al [38]. Hardness value for 1200 rpm processed sample was observed to be 72 HV, which was the lowest compared to 84 HV at 1000 rpm and 95 HV at 800 rpm.

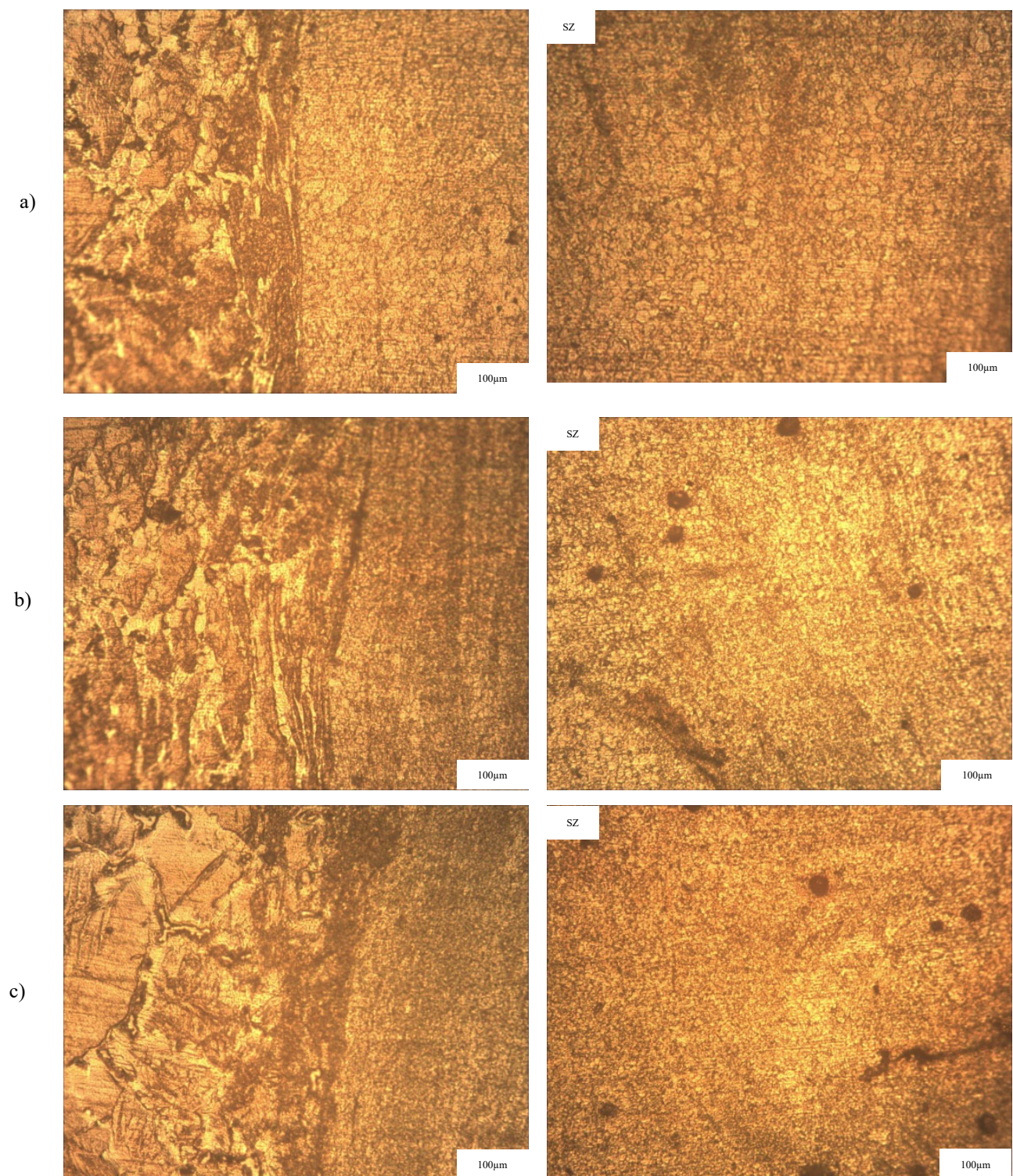


Fig. 6. Microstructure at 200 X for interface and stir zone of FSPed specimen processed: a) at 800 rpm, b) at 1000 rpm, c) at 1200 rpm

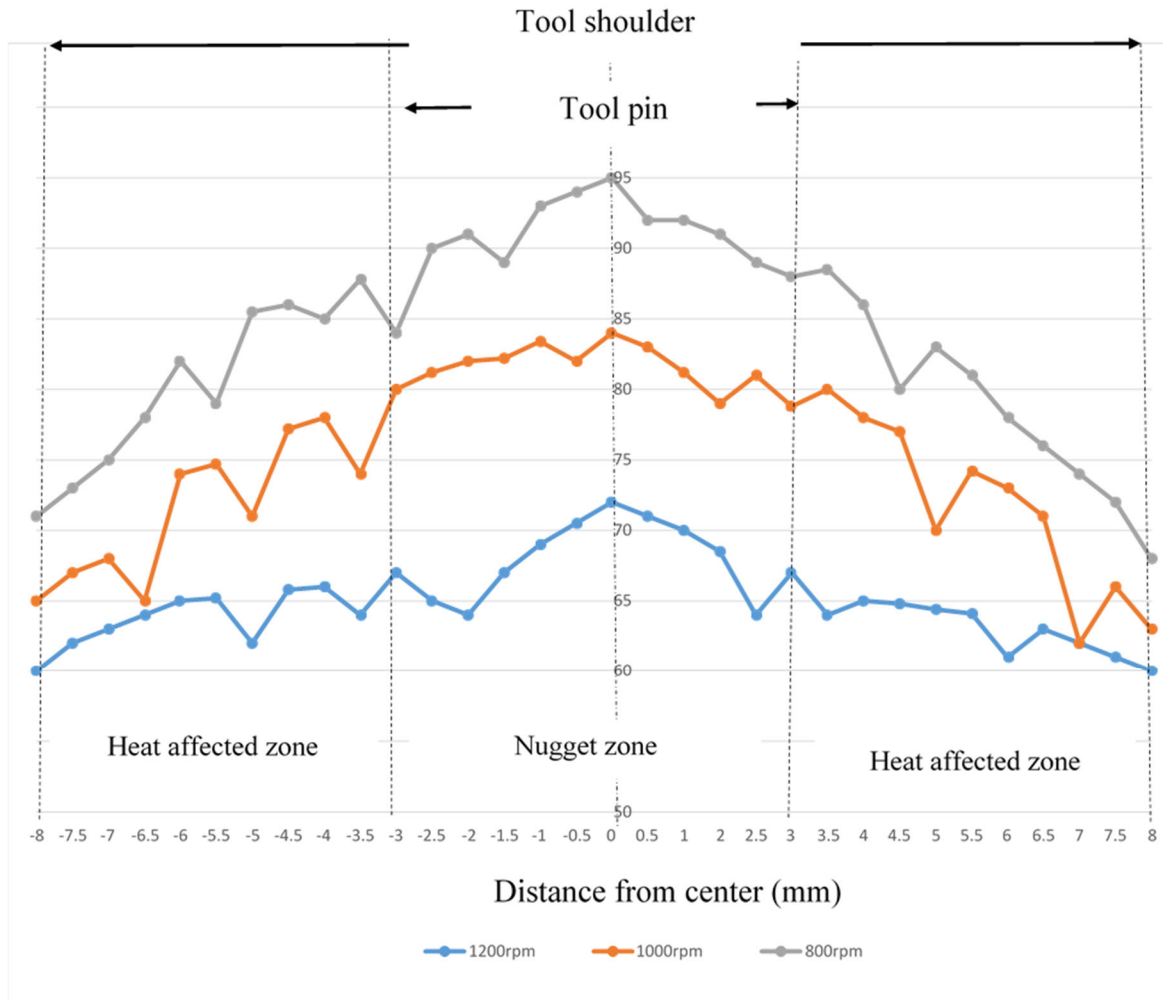


Fig. 7. Hardness values for FSPed composites processed at different tool rotation speed

### 3.2. Wear performance

Final values of wear rate were calculated with respect to the sliding distance. In addition, entire values for the composite along with the base material considering varying load are presented in tabular form in Table 4.

Figures 8 and 9, shows that the specimen processed at 800 rpm shows lower value of height loss with respect to time as contrasted with composite developed at 1000 rpm, 1200 rpm and the base metal. This may be attributed to low tool rotational speed producing smaller grains, higher hardness resulting in lesser wear [30,39]. In spite of low value of hardness for FSPed, the sample processed at 1200 rpm had, lower value of wear rate and low height loss was observed due to more homogenous distribution of nanoparticles in consensus with Azizieh et. al [23].

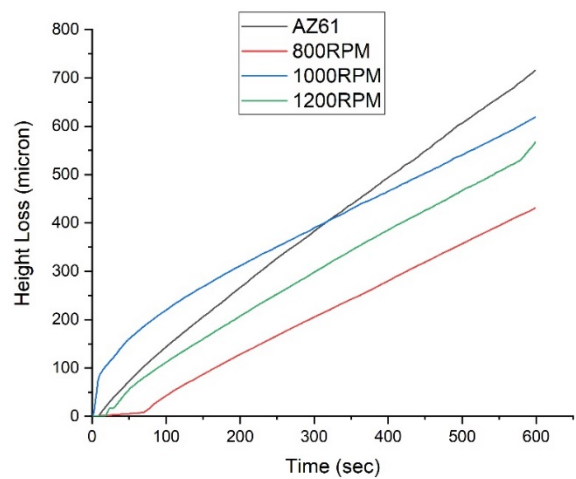


Fig. 8. Height loss of all specimens with respect to time at 10 N

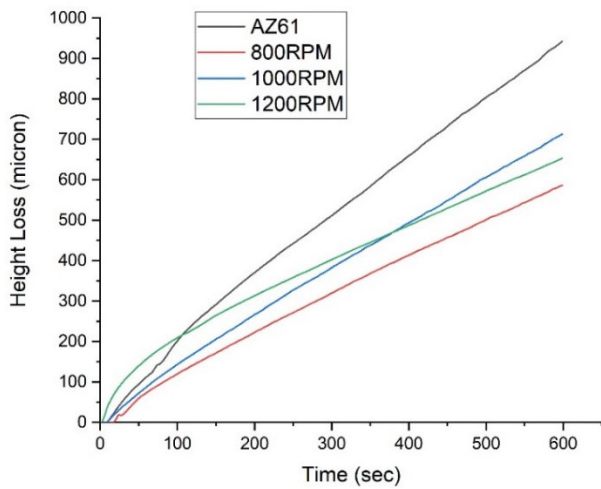


Fig. 9. Height loss of all specimens with respect to time at 20 N

Plots shown in Figure 10, represents findings of wear rate comparison between AZ61A base metal and FSPed processed composites examined at various FSP parameters and tribological loads. As was observed in Figure 8, the magnesium base AZ61A metal wear rate was high compared to the processed composites.

As observed in Figure 10, with increase in applied load, the wear rate increases for both base metal and developed composites, which is in agreement with the Archard's wear equation [40]. However, at an elevated value of load, wear rate for the base metal increases sharply as shown in Figure 10, which reflects mild to severe delamination of the surface, also reported by Ram et. al [22]. Apparent changes take place in wear rate of metal matrix composites (MMCs) at

increased load and it shows lower values of wear rate compared to the base metal. In other words, wear resistance is comparatively high for developed composites at high load. In FSP samples, refined grains and uniformly distributed secondary phase particles results in hardened surface which has also been reported by various researchers [34, 41-46]. This low wear rate and resistance to wear be due to the (a) addition of secondary phase particles develops enhanced values of hardness for FSP composite, (b) additive TiC particulate content not only minimizes the contact area of composite and counter surface, additionally it opposes the cutting activity of the counterface adequately (c) grain boundary and secondary phase mechanism i.e. Hall-pitch and Orowan mechanism contributes in development of hardness and strength of composite, resulting in greater load bearing capacity.

### 3.3. Coefficient of friction

Amplitude of friction coefficient to the function of time for base metal and for composites samples are shown in Figure 11. The friction coefficient fluctuations for initial time frame is extremely high, which might be due to the new disc surface introduction to the pin. To obtain precise values and to remove the material stored on plate, steel disc was cleaned before each run. As observed in Figure 11, at 10 N higher variations are obtained for all specimens. However, extensive variation in friction coefficient with high amplitudes for base metal at 10 N is noticed while these progressions for FSPed composites were not all that broad. Mainly this fluctuation is an outcome of adhesion of the pin to counterside. Moreover SEM images also suggests that abrasive wear also occurs. Therefore, at 10 N adhesive wear

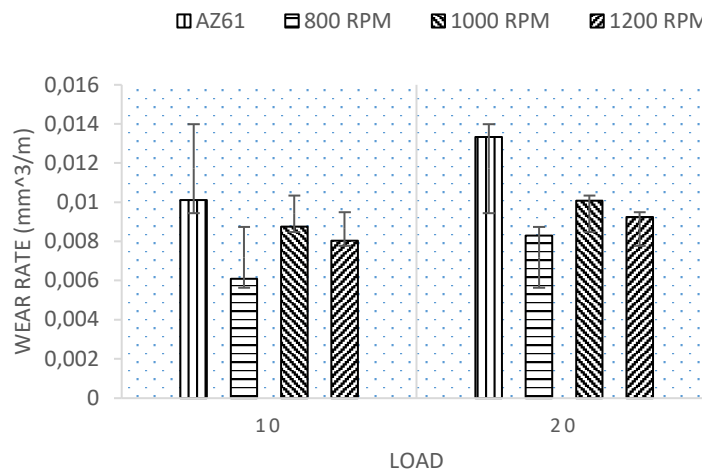


Fig. 10. Wear rate plots of base metal AZ61A and FSPed composites

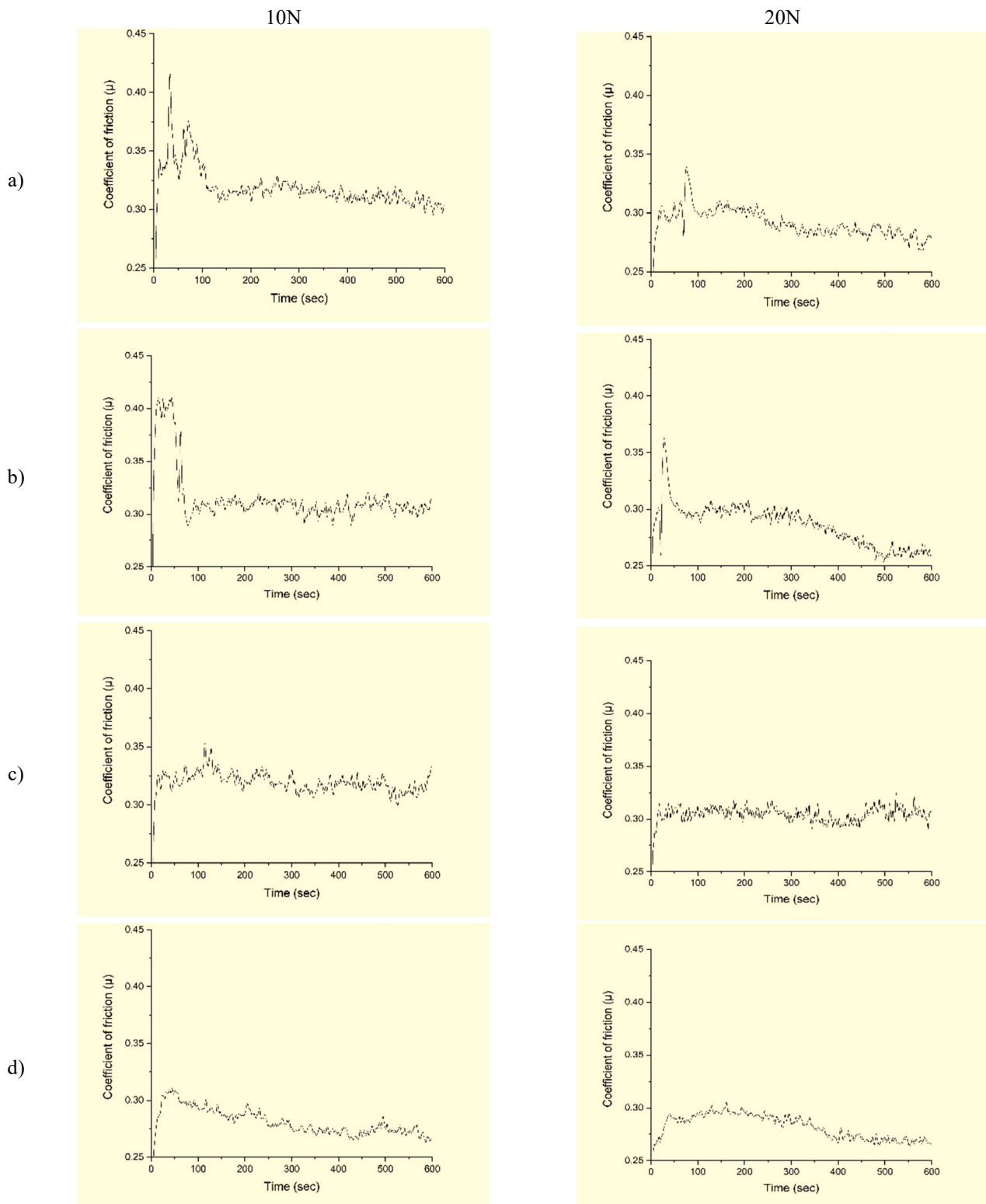


Fig. 11. Coefficient of friction values with respect to time a) for base metal AZ61A b) for FSPed specimen processed at 800 rpm c) for FSPed specimen processed at 1000 rpm. d) for FSPed specimen processed at 1200 rpm

mechanism is dominant consequently develops higher values of friction coefficient for base metal when compared to developed composites. In subsequent samples distribution of TiC particles acted as thin film and gives rise to selective material removal, hence decrease the mean friction coefficient as can be seen in Figure 12. As friction coefficient reduced, the actuating shear stress on the sliding surface decreases and results in resistance to wear. In case of FSPed composites processed at 1200 rpm in spite of low hardness values, it is uniform distribution of particles that leads it to homogeneity, which prevents large variation in friction coefficient.

When load increases, the variations in fluctuation decreases in all specimens as shown in Figure 11. Also, the base metal mean friction coefficient of all FSPed composites decreased as the applied load increased. This may be attributed to high thermal energy developed, which softened the materials. Additionally for FSPed specimens, mixing of secondary phase particles minimize the direct contact area and direct contact load, hence decrease in the friction coefficient was noticed. This behaviour can also be ascribed to hardness. Therefore, at low applied load hardness is acting as a prevailing variable. In any case, at enhanced load values, friction coefficient was mainly influenced by wear mechanism i.e. delamination. Therefore, the composite with low friction coefficient worn less which is in agreement with Lu et al. [47].

### 3.4. Wear mechanism

SEM micrographs of the as received AZ61A and FSPed samples were taken to investigate the morphology of the worn surfaces and included in Figures 13 and 14. As can be observed in Figures 13 and 14, the surface of base metal

AZ61A shows straight deep plows/grooves. This may be attributed to frictional heat that breaks into the initial network of magnesium like  $\beta\text{-Mg}_{17}\text{Al}_{12}$ . This brittle and coarse phase shows its inability to effectively act as an obstacle to wear, consequently it softening of the material. Additionally this heat generates good amount of plastic deformation, which leads to the formation of deep grooves. The presence of these deep grooves could also be brought about by microploughing, a sub mechanics of abrasion. Also, the appearance of scratches on the base metal surface shows some evidence of abrasive wear. For base metal, a range of adhesive and abrasive wear was observed which is in conjunction with [17,23]. However, deep grooves indicate severe adhesive wear and its domination, consequently debris formed and massive surface damage on pin surface was found. This may be also be related to lower value hardness for base material as contrasted to FSPed composites. When applied load increase to 20N it is evident from Figure 12 that base metal forms more cracks and has widened grooves.

As is shown in Figures 13 and 14, the wear component in the composite is unique and different compared with the base metal. Uniform grains and homogenous distribution of TiC particles decidedly influenced the wear resistance. EDS images also validates the presence of TiC particles in almost all the MMCs. Also the addition of TiC particles in the base metal, a) minimized contact area of metal and counter part b) minimized direct load, which lead to change in the severe wear to mild wear. For all manufactured composites, thus, the abrasive wear mechanism was found to be the dominant wear mechanism by the loose debris particles. These loose debris particles mainly shows up due to oxidizing MMCs and pulling of TiC during sliding.

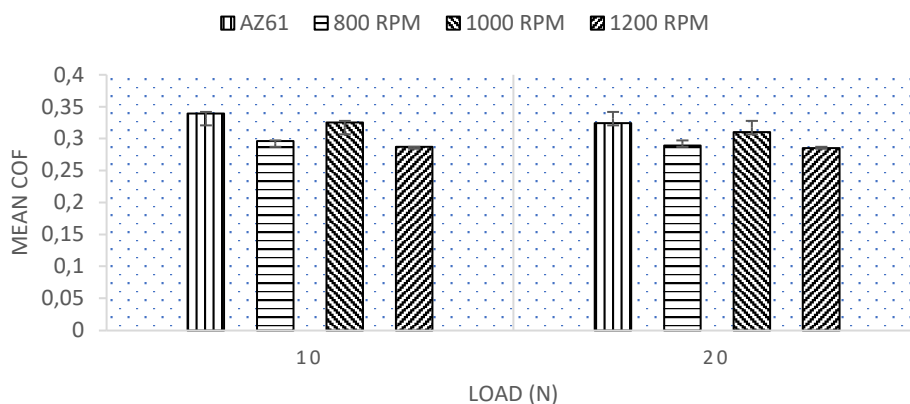


Fig. 12. Values of mean coefficient of friction as a function of load

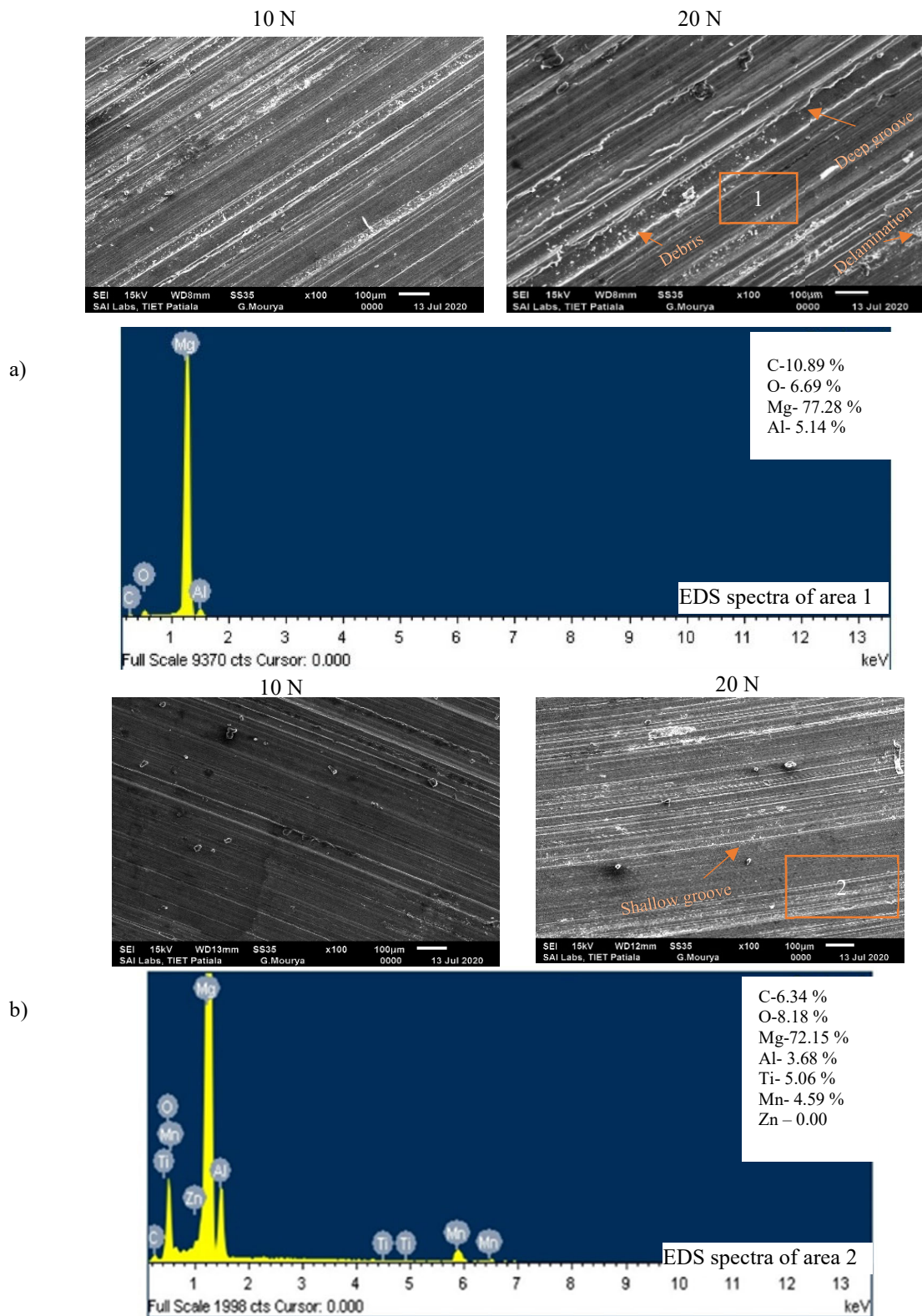


Fig. 13. SEM micrographs and corresponding EDS of worn surfaces; a) for base metal AZ61A, b) for FSPed specimen processed at 800 rpm

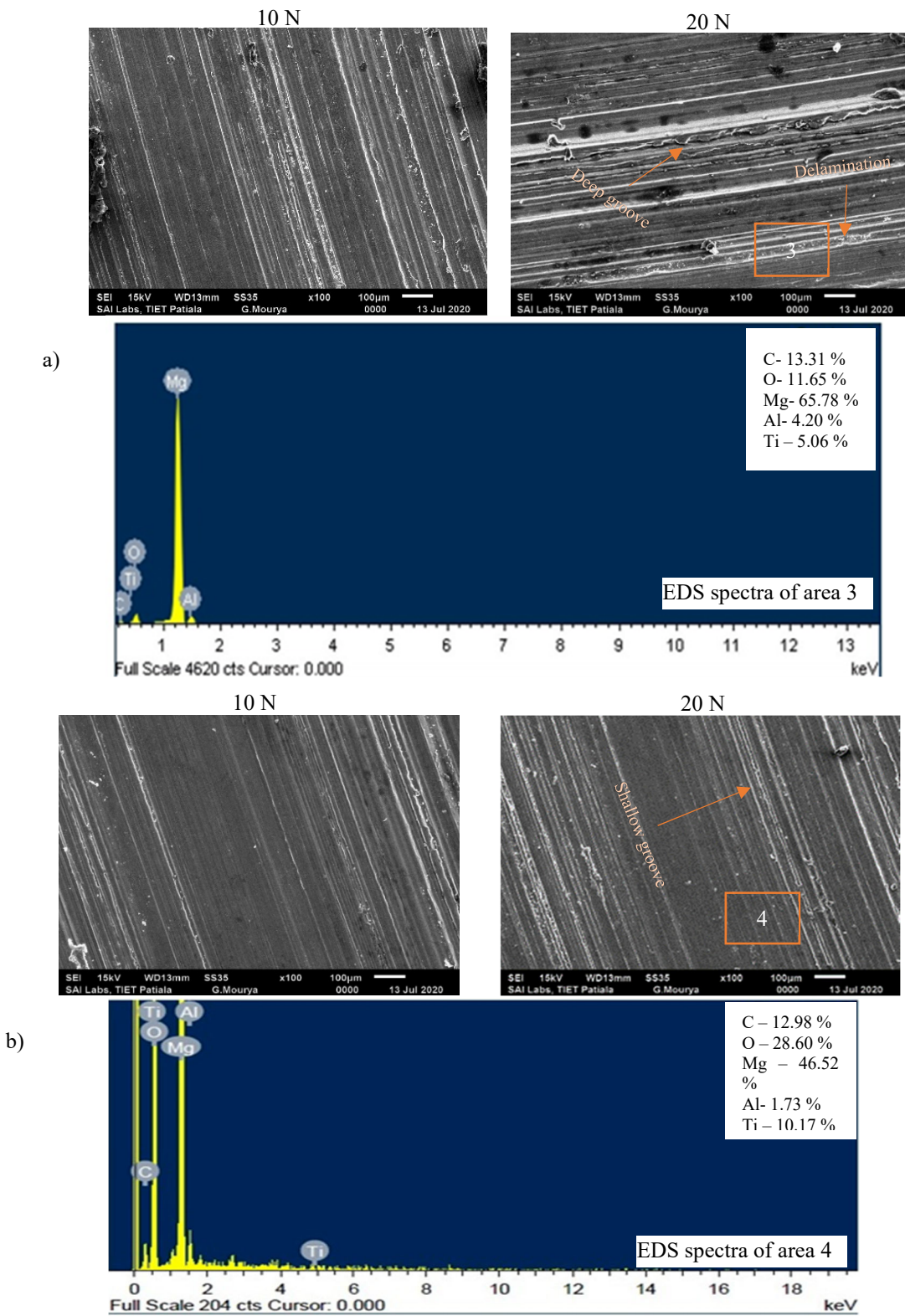


Fig. 14. SEM micrographs and corresponding EDS of worn surfaces; a) for FSPed specimen processed at 1000 rpm, b) for FSPed specimen processed at 1200 rpm

Generally, enhanced load creates frictional heating that causes changes in morphology of worn surfaces from fine scratches to grooves. However, FSPed composite surface processed at 1200 rpm showed microcracks that may be due to good nanoparticle distribution, which reduced the immediate contact load and thus forestalled the delamination. It merits referencing that for the specimen processed at 1000 rpm and 10 N or 20 N delamination of the MMCs layers was likewise found in some places. However, at 1200 rpm and 10 N metal matrix layer delamination was observed to be diminished.

#### 4. Conclusions

In this work magnesium, based AZ61A/TiC composites were effectively manufactured utilizing FSP. The tribological characteristics of the as-got AZ61A and fabricated composites were examined. The main findings of the examination can be summed up as follows:

1. Presence of secondary phase TiC particles and grain refinement directly influenced hardness and wear rate of the composites.
2. Enhanced hardness was achieved for composite fabricated at 800 rpm i.e. 95 HV which is way too high as contrasted to the hardness of AZ61A base metal i.e. 60 HV.
3. For composites, a lower wear rate was observed compared to base metal that may be attributed to increased hardness values.
4. For lower value of loads, composites showed lower friction coefficients due to reinforced particles load bearing abilities.
5. Worn surface morphology was greatly influenced by tool rotational speeds. Due to high hardness and uniform particle distribution of specimen prepared at 800 rpm and 1200 rpm, worn surface appeared to be smooth with few shallow grooves.

#### Acknowledgements

The authors would like to thank I.K. Gujral Punjab Technical University, Kapurthala, India for giving us the opportunity to carry on this research work. Also authors are highly thankful to Dr Pavel Somavat, A.P, University of Texas, USA for his valuable suggestions.

#### References

- [1] M. Gupta, N. Sharon, Magnesium, Magnesium alloys and magnesium composites, J. Wiley and Sons, 2010.
- [2] I. Mukhin, E. Perevezentsev, O. Palashov, Fabrication of Composite Laser Elements by a New Thermal Diffusion Bonding Method, *Optical Materials Express* 4/2 (2014) 266-271. DOI: <https://doi.org/10.1364/OME.4.000266>
- [3] A.K. Bodukuri, K. Eswaraiyah, K. Rajendar, V. Sampath, Fabrication of Al-SiC-B<sub>4</sub>C Metal Matrix Composite by Powder Metallurgy Technique and Evaluating Mechanical Properties, *Perspectives in Science* 8 (2016) 428-431. DOI: <https://doi.org/10.1016/j.pisc.2016.04.096>
- [4] Q.C. Jiang, H.Y. Wang, B.X. Ma, Y. Wang, F. Zhao, Fabrication of B<sub>4</sub>C Particulate Reinforced Magnesium Matrix Composite by Powder Metallurgy, *Journal of Alloys and Compounds* 386/1-2 (2005) 177-181. DOI: <https://doi.org/10.1016/j.jallcom.2004.06.015>
- [5] Th. Schubert, B. Trindade, T. Weißgärber, B. Kieback. Interfacial Design of Cu-Based Composites Prepared by Powder Metallurgy for Heat Sink Applications, *Materials Science and Engineering: A* 475/1-2 (2008) 39-44. DOI: <https://doi.org/10.1016/j.msea.2006.12.146>
- [6] X. Wang, A. Jha, R. Brydson, In Situ Fabrication of Al<sub>3</sub>Ti Particle Reinforced Aluminium Alloy Metal-Matrix Composites, *Materials Science and Engineering: A* 364/1-2 (2004) 339-345. DOI: <https://doi.org/10.1016/j.msea.2003.08.049>
- [7] B. Yang, F. Wang, J.S. Zhang, Microstructural Characterization of in Situ TiC/Al and TiC/Al-20Si-5Fe-3Cu-1Mg Composites Prepared by Spray Deposition, *Acta Materialia* 51/17 (2003) 4977-4989. DOI: [https://doi.org/10.1016/S1359-6454\(03\)00292-1](https://doi.org/10.1016/S1359-6454(03)00292-1)
- [8] J. Hashim, L. Looney, M.S.J. Hashmi, Metal matrix composites : production by the stir casting method, *Journal of Materials Processing Technology* 92-93 (1999) 1-7. DOI: [https://doi.org/10.1016/S0924-0136\(99\)00118-1](https://doi.org/10.1016/S0924-0136(99)00118-1)
- [9] H. Uozumi, K. Kobayashi, K. Nakanishi, T. Matsunaga, K. Shinozaki, H. Sakamoto, T. Tsukada, C. Masuda, M. Yoshida, Fabrication Process of Carbon Nanotube/Light Metal Matrix Composites by Squeeze Casting, *Materials Science and Engineering: A* 495/1-2 (2008) 282-287. DOI: <https://doi.org/10.1016/j.msea.2007.11.088>
- [10] H. Hu, Squeeze Casting of Mg Alloy and Their Composites, *Journal of Materials Science* 33 (1998) 1579-1589. DOI: <https://doi.org/10.1023/A:1017567821209>
- [11] M. Dhanashekar, V.S. Senthil Kumar, Squeeze casting of aluminium metal matrix composites – an overview, *Procedia Engineering* 97 (2014) 412-420. DOI: <https://doi.org/10.1016/j.proeng.2014.12.265>

- [12] C.N. He, N.Q. Zhao, C.S. Shi, S.Z. Song, Mechanical Properties and Microstructures of Carbon Nanotube-Reinforced Al Matrix Composite Fabricated by in Situ Chemical Vapor Deposition, *Journal of Alloys and Compounds* 487/1-2 (2009) 258-262. DOI: <https://doi.org/10.1016/j.jallcom.2009.07.099>
- [13] P. Delhaes, Chemical Vapor Deposition and Infiltration Processes of Carbon Materials, *Carbon* 40/5 (2002) 641-657. DOI: [https://doi.org/10.1016/S0008-6223\(01\)00195-6](https://doi.org/10.1016/S0008-6223(01)00195-6)
- [14] R.S. Mishra, Z.Y. Ma, Friction Stir Welding and Processing, *Materials Science and Engineering R: Reports* 50/1-2 (2005) 1-78. DOI: <https://doi.org/10.1016/j.mser.2005.07.001>
- [15] H.S. Arora, H. Singh, B.K. Dhindaw, Composite Fabrication Using Friction Stir Processing – a Review, *International Journal of Advanced Manufacturing Technology* 61/9-12 (2012) 1043-1055. DOI: <https://doi.org/10.1007/s00170-011-3758-8>
- [16] V. Sharma, U. Prakash, B.V. Manoj Kumar, Surface Composites by Friction Stir Processing : A Review *Journal of Materials Processing Technology* 224 (2015) 117-134. DOI: <https://doi.org/10.1016/j.jmatprotec.2015.04.019>
- [17] G. Madhusudhan Reddy, A. Sambasiva Rao, K. Srinivasa Rao, Friction Stir Processing for Enhancement of Wear Resistance of ZM21 Magnesium Alloy, *Transactions of the Indian Institute of Metals* 66/1 (2013) 13-24. DOI: <https://doi.org/10.1007/s12666-012-0163-4>
- [18] M. Abbasi, B. Bagheri, M. Dadaei, H.R. Omidvar, M. Rezaei, The Effect of FSP on Mechanical, Tribological, and Corrosion Behavior of Composite Layer Developed on Magnesium AZ91 Alloy Surface, *International Journal of Advanced Manufacturing Technology* 77/9-12 (2015) 2051-2058. DOI: <https://doi.org/10.1007/s00170-014-6577-x>
- [19] J. Singh, H. Lal, N. Bala, Investigations on the wear behaviour of friction stir processed magnesium based AZ91 alloy, *International Journal of Mechanical Engineering and Robotics Research* 2/3 (2013) 271-274.
- [20] H.S. Arora, H. Singh, B.K. Dhindaw, H.S. Grewal, Improving the Tribological Properties of Mg Based AZ31 Alloy Using Friction Stir Processing, *Advanced Materials Research* 585 (2012) 579-583. DOI: <https://doi.org/10.4028/www.scientific.net/AMR.585.579>
- [21] H.S. Arora, H. Singh, B.K. Dhindaw, Wear Behaviour of a Mg Alloy Subjected to Friction Stir Processing, *Wear* 303/1–2 (2013) 65-77. DOI: <https://doi.org/10.1016/j.wear.2013.02.023>
- [22] B. Ram, D. Deepak, N. Bala, Role of Friction Stir Processing in Improving Wear Behavior of Mg/SiC Composites Produced by Stir Casting Route, *Materials Research Express* 6/2 (2019) 026577. DOI: <https://doi.org/10.1088/2053-1591/aaf1e4>
- [23] M. Azizieh, A.N. Larki, M. Tahmasebi, M. Bavi, E. Alizadeh, H.S. Kim. Wear Behavior of AZ31/Al<sub>2</sub>O<sub>3</sub> Magnesium Matrix Surface Nanocomposite Fabricated via Friction Stir Processing, *Journal of Materials Engineering and Performance* 27/4 (2018) 2010-2017. DOI: <https://doi.org/10.1007/s11665-018-3277-y>
- [24] G. Faraji, P. Asadi, Characterization of AZ91/Alumina Nanocomposite Produced by FSP, *Materials Science and Engineering: A* 528/6 (2011) 2431-2440. DOI: <https://doi.org/10.1016/j.msea.2010.11.065>
- [25] I. Dinaharan, S.C. Vettivel, M. Balakrishnan, E.T. Akinlabi, Influence of Processing Route on Microstructure and Wear Resistance of Fly Ash Reinforced AZ31 Magnesium Matrix Composites, *Journal of Magnesium and Alloys* 7/1 (2019) 155-165. DOI: <https://doi.org/10.1016/j.jma.2019.01.003>
- [26] H. Patle, B. Ratna Sunil, R. Dumpala, Sliding Wear Behavior of AZ91/B<sub>4</sub>C Surface Composites Produced by Friction Stir Processing, *Materials Research Express* 7/1 (2020) 016586. DOI: <https://doi.org/10.1088/2053-1591/ab6a55>
- [27] W.A. Monteiro, S.J. Buso, L.V. Silva, Application of Magnesium Alloys in Transport, in: W.A. Monteiro (ed.), *New Features on Magnesium Alloys*, IntechOpen, 1998, 1-14. DOI: <https://doi.org/10.5772/48273>
- [28] C.-C. Lin, S.-J. Huang, C.-C. Liu, Structural analysis and optimization of bicycle frame designs, *Advances in Mechanical Engineering* 9/12 (2017) 1-10. DOI: <https://doi.org/10.1177/1687814017739513>
- [29] Weblinks: Magnesium Applications. Available from: [https://www.tms.org/Communities/FTAttachments/Mg%20Applications\\_Corporate.pdf](https://www.tms.org/Communities/FTAttachments/Mg%20Applications_Corporate.pdf)
- [30] S. Sharma, A. Handa, S.S. Singh, D. Verma, Synthesis of a Novel Hybrid Nanocomposite of AZ31Mg-Graphene-MWCNT by Multi-Pass Friction Stir Processing and Evaluation of Mechanical Properties, *Materials Research Express* 6/12 (2019) 126531. DOI: <https://doi.org/10.1088/2053-1591/ab54da>
- [31] A.P. Sekhar, D. Das, Influence of Artificial Aging on Mechanical Properties and High Stress Abrasive Wear Behaviour of Al-Mg-Si Alloy, *Metals and Materials International* (2019). DOI: <https://doi.org/10.1007/s12540-019-00399-9>
- [32] J.A. Valle, Friction Stir Processing of the Magnesium Alloy AZ61: Grain Size Refinement and Mechanical

- Properties, Materials Science Forum 706-709 (2012) 823-1828. DOI: <https://doi.org/10.4028/www.scientific.net/MSF.706-709.1823>
- [33] D. Khayyamin, A. Mostafapour, R. Keshmiri, The Effect of Process Parameters on Microstructural Characteristics of AZ91/SiO<sub>2</sub> Composite Fabricated by FSP, Materials Science and Engineering: A 559 (2013) 217-221. DOI: <https://doi.org/10.1016/j.msea.2012.08.084>
- [34] S. Das, R.S. Mishra, K.J. Doherty, K.C. Cho, B. Davis, R. DeLorme, Magnesium Based Composite Via Friction Stir Processing., in: R. Mishra, M.W. Mahoney, Y. Sato, Y. Hovanski, R. Verma (eds), Friction Stir Welding and Processing VII, Springer, Cham, 245-252. DOI: [https://doi.org/10.1007/978-3-319-48108-1\\_25](https://doi.org/10.1007/978-3-319-48108-1_25)
- [35] G. Vedabouriswaran, S. Aravindan, Development and characterization studies on magnesium alloy (RZ 5) surface metal matrix composites through friction stir processing, Journal of Magnesium and Alloys 6/2 (2018) 145-163. DOI: <https://doi.org/10.1016/j.jma.2018.03.001>
- [36] D. Ahmadkhaniha, M. Heydarzadeh Sohi, A. Salehi, R. Tahavvori, Formations of AZ91/Al<sub>2</sub>O<sub>3</sub> nanocomposite layer by friction stir processing, Journal of Magnesium and Alloys 4/4 (2016) 314-318. DOI: <https://doi.org/10.1016/j.jma.2016.11.002>
- [37] M. Azizieh, H.S. Kim, A.H. Kokabi, P. Abachi, B.K. Shahraki, Fabrication of AZ31/Al<sub>2</sub>O<sub>3</sub> nanocomposites by friction stir processing, Reviews on Advanced Materials Science 28/1 (2011) 85-89.
- [38] R. Sathiskumar, I. Dinaharan, N. Murugan, S.J. Vijay, Influence of Tool Rotational Speed on Microstructure and Sliding Wear Behavior of Cu/B<sub>4</sub>C Surface Composite Synthesized by Friction Stir Processing, Transactions of Nonferrous Metals Society of China 25/1 (2014) 95-102. [https://doi.org/10.1016/S1003-6326\(15\)63583-X](https://doi.org/10.1016/S1003-6326(15)63583-X)
- [39] P. Asadi, M.K. Besharati Givi, G. Faraji, Producing Ultrafine-Grained AZ91 from as-Cast AZ91 by FSP, Materials and Manufacturing Processes 25/11 (2010) 1219-1226. DOI: <https://doi.org/10.1080/10426911003636936>
- [40] J.F. Archard, Contact and rubbing of flat surfaces, Journal of Applied Physics 24/8 (1953) 981-988. DOI: <https://doi.org/10.1063/1.1721448>
- [41] G. Faraji, O. Dastani, S. Ali Asghar, A. Mousavi. Effect of Process Parameters on Microstructure and Micro-Hardness of AZ91/Al<sub>2</sub>O<sub>3</sub> Surface Composite Produced by FSP, Journal of Materials Engineering and Performance 20 (2011) 1583-1590. DOI: <https://doi.org/10.1007/s11665-010-9812-0>
- [42] M. Dadashpour, A. Mostafapour, R. Yeşildal, S. Rouhi. Effect of Process Parameter on Mechanical Properties and Fracture Behavior of AZ91C/SiO<sub>2</sub> Composite Fabricated by FSP, Materials Science and Engineering: A 655 (2016) 379-387. DOI: <https://doi.org/10.1016/j.msea.2015.12.103>
- [43] M. Azizieh, A.H. Kokabi, P. Abachi, Effect of Rotational Speed and Probe Profile on Microstructure and Hardness of AZ31/Al<sub>2</sub>O<sub>3</sub> Nanocomposites Fabricated by Friction Stir Processing, Materials and Design 32/4 (2011) 2034-2041. DOI: <https://doi.org/10.1016/j.matdes.2010.11.055>
- [44] M. Navazani, K. Dehghani, Investigation of Microstructure and Hardness of Mg/TiC Surface Composite Fabricated by Friction Stir Processing (FSP), Procedia Materials Science 11 (2015) 509-514. DOI: <https://doi.org/10.1016/j.mspro.2015.11.082>
- [45] R. Bauri, G.D. Janaki Ram, D. Yadav, C.N. Shyam Kumar, Effect of Process Parameters and Tool Geometry on Fabrication of Ni Particles Reinforced 5083 Al Composite by Friction Stir Processing, Materials Today: Proceedings 2/4-5 (2015) 3203-3211. DOI: <https://doi.org/10.1016/j.matpr.2015.07.115>
- [46] M. Zohoor, M.K. Besharati Givi, P. Salami, Effect of Processing Parameters on Fabrication of Al-Mg/Cu Composites via Friction Stir Processing, Materials and Design 39 (2012) 358-365. DOI: <https://doi.org/10.1016/j.matdes.2012.02.042>
- [47] D. Lu, Y. Jiang, R. Zhou, Wear Performance of Nano-Al<sub>2</sub>O<sub>3</sub> Particles and CNTs Reinforced Magnesium Matrix Composites by Friction Stir Processing, Wear 305/1-2 (2013) 286-290. DOI: <https://doi.org/10.1016/j.wear.2012.11.079>



© 2020 by the authors. Licensee International OCSCO World Press, Gliwice, Poland. This paper is an open access paper distributed under the terms and conditions of the Creative Commons Attribution-NonCommercial-NoDerivatives 4.0 International (CC BY-NC-ND 4.0) license (<https://creativecommons.org/licenses/by-nc-nd/4.0/deed.en>).